Available online at www.sciencedirect.com

ScienceDirect

Acta Materialia 56 (2008) 3982–3989

Acta MATERIALIA

www.elsevier.com/locate/actamat

Structural effect of fullerene derivative on polaron relaxation and charge transfer in poly(3-hexylthiophene)/fullerene composite

V.I. Krinichnyi *, P.A. Troshin, N.N. Denisov

Institute of Problems in Chemical Physics, Semenov Avenue 1, Chernogolovka 142432, Russia

Received 3 January 2008; received in revised form 11 April 2008; accepted 13 April 2008
Available online 20 May 2008

Abstract

The structural effect of a side chain in a fullerene derivative on electron relaxation and polaronic charge transfer in a poly(3-hexylthiophene)/fullerene composite was studied by 3 cm waveband electron paramagnetic resonance. All the systems with different fullerene derivatives demonstrate a sum spectrum of small localized and mobile polarons whose contributions depend on the structure of the fullerene derivative. Both the spin–lattice and spin–spin relaxation times were determined separately in a wide (77–320 K) temperature region using the steady-state saturation method. It was shown that spin relaxation, susceptibility and dynamics are governed by the dipole–dipole interaction of the polarons as well as by the structure of the side chains in the fullerene derivative. The treatment of the polymer matrix by the fullerene changes its dimensionality and accelerates polaron diffusion along polymer chains.

Keywords: Electron paramagnetic resonance; Polythiophene and derivatives; Fullerene; Polaron; Relaxation

1. Introduction

Conjugated polymers with extended π-electron systems in their main chain attract much interest from not only purely scientific viewpoints but also because of their prospective use as a flexible active matrix for new electronic devices such as light emitting diodes [1], solar cells [2,3] and thin film field effect transistors [4]. The understanding of the basic physics underlying the electrical, thermal and optical behavior of organic polymeric materials is essential for the optimization of devices fabricated using these materials.

Among side chain substituted polymers, the alkyl-substituted polythiophenes [5] are seen as a major milestone in the development of high-performance solution processible electronic polymer systems. As the parent polymer, polythiophene, already tends towards backbone planarity, there is a strong cooperative self-assembly of poly(3-alkylthiophenes) (P3AT) into well-ordered lamellar phases [6,7]. For some applications, this behavior has the desirable effect of enhancing interchain *p*-orbital overlap, thereby improving the electron transport properties. Such overlapping is higher in poly(3-hexylthiophene) (P3HT) with shorter alkyl substitute, which stipulates faster polaron formation and recombination in this polymer. The nature of the coupling between adjacent alkylthiophene rings in P3HT determines its optical, transport and electronic properties. For example, the steric repulsion between the sulfur atoms and the hexyl side groups in head-to-head conformations causes torsion in the polythiophene backbone out of planarity, and hence a decrease in the conjugation of the π-conjugated system [8]. This effect changes the electronic band structure of the polymer and leads to novel photoluminescence and electroluminescence [9]. Head-to-tail regioregular P3HT exhibits a planar configuration, higher mobility and a higher degree of crystallinity in the films [10]. Real P3AT are characterized by weak paramagnetism due to mobile polarons originating from the synthesis and/or the adsorption of oxygen from the ambient atmosphere [11]. The illumination of a

---

* Corresponding author.

E-mail addresses: kivi@cat.icp.ac.ru, kivirus@gmail.com (V.I. Krinichnyi).

1359-6454/$34.00 © 2008 Acta Materialia Inc. Published by Elsevier Ltd. All rights reserved.
doi:10.1016/j.actamat.2008.04.020

polymer/fullerene film by light leads to the photoinduced electron transfer from the polymer chain to the fullerene molecule and, therefore, to simultaneous formation of additional polarons P^+ and fullerene ion-radicals C_{60}^{-} in the film. The efficiency of such a process, including the charge separation, quantum yield, absence of the electron traps, etc. should be governed by the structure of both the polymer and the fullerene derivative. P3HT and fullerene derivatives are frequently used as effective donor and acceptor composite materials in plastic solar cells [12–14]. Undoubtedly, the charge transfer in the initial and fullerene-treated polymers should be studied before their use as the active matrix of solar cells. However, the physics processes in these systems have been scarcely studied and understood.

Polarons stabilized in P3AT possess spin $\frac{1}{2}$, so electron paramagnetic resonance (EPR) is a powerful method for the study of such solids [11,15,16]. As in the case of other organic solids, the method allows one to determine the main magnetic resonance parameters through the measurement of the paramagnetic susceptibility, g-factor, linewidth and line shape of the polarons, and new important information on the amplitude and correlation time of inside fluctuating fields in fullerene-modified P3AT compounds from longitudinal T_1 and transversal T_2 electron spin relaxation times. Spin–spin relaxation time is usually measured from the EPR linewidth; however, inhomogeneous broadening masks increase the effect of fluctuating fields.

The main aim of this paper is to clarify the role of the structure of the fullerene derivative in the magnetic, relaxation and dynamics properties of a whole spin reservoir in the polymer/fullerene system. The existence of polarons with different relaxation and mobility in P3HT blended with fullerene derivatives is shown. The effective relaxation times and paramagnetic susceptibility of these paramagnetic reservoirs were studied, as well as the dynamics of mobile polarons in a wide temperature range, and the effect of the dipole–dipole interaction between mobile and localized spins on these parameters was analyzed. Finally, the correlation between the electronic and macromolecular properties was analyzed. Small polarons are formed in the initial and fullerene-modified P3HT whose main magnetic and electronic properties are governed by the structure of the fullerene derivative. The dimensionality of the polymer/fullerene system was also determined by the structure of the fullerene derivative.

2. Experimental

Regioregular P3HT (the chemical structure is shown in Fig. 1) with lattice constants $a = 1.680$ nm, $b = 0.766$ nm, and $c = 0.770$ nm [7] was purchased from Aldrich and used without further purification. The synthesis of the soluble fullerene derivatives **1–6**

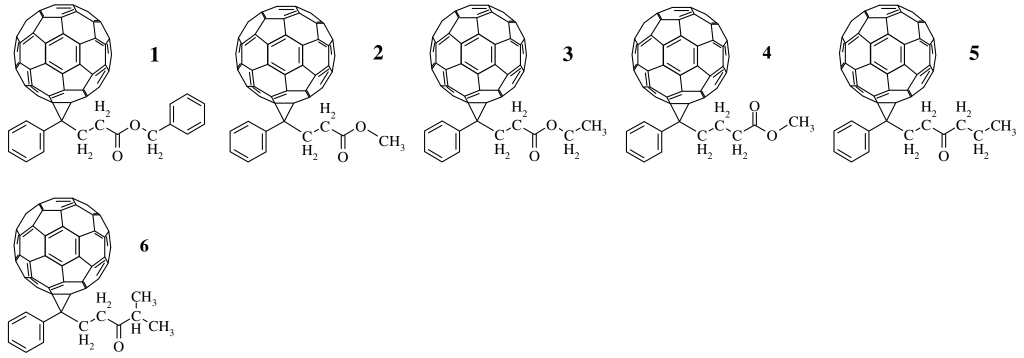

with side chains $R \equiv -(CH_2)_2C(O)OCH_2Ph$, $-(CH_2)_2C(O)O-CH_3$, $-(CH_2)_2C(O)OCH_2CH_3$, $-(CH_2)_3C(O)OCH_3$, $-(CH_2)_2C(O)O(CH_2)_2CH_3$, $-(CH_2)_2C(O)OCH(CH_3)_2$, respectively, was described in detail previously [17]. The chlorobenzene solution of P3HT and appropriate fullerene derivatives **1–6** (1:1 wt. ratio) with concentration ~1 wt.% was placed onto a ceramic plane and dried, so that the respective composites P3HT/**1**, P3HT/**2**, P3HT/**3**, P3HT/**4**, P3HT/**5** and P3HT/**6** were formed as film $\sim 4 \times 8$ mm^2 in area and ~0.1 mm thick.

EPR study of these samples was performed using a 3 cm (X-band, 9.7 GHz) PS-100X spectrometer with 100 kHz field AC modulation for phase-lock detection. The temperature of the sample was stabilized in a nitrogen atmosphere by the BRT-IOH controller in the range 90–320 K with ±0.5° error. In addition, the spectra of the samples were also registered at 77 K in quartz dewar with liquid nitrogen. The total paramagnetic susceptibility of the samples was determined by comparing their double integrated EPR spectra with that of a calibrated quantity of 1,1-diphenyl-2-picrylhydrazyl. EPR spectra were simulated using the Bruker WinEPR SimFonia V.1.25 program. The uncertainty in the determination of the peak-to-peak linewidth ΔB_{pp} and the value of the g-factor were consequently $\pm 2 \times 10^{-2}$ G and $\pm 2 \times 10^{-4}$.

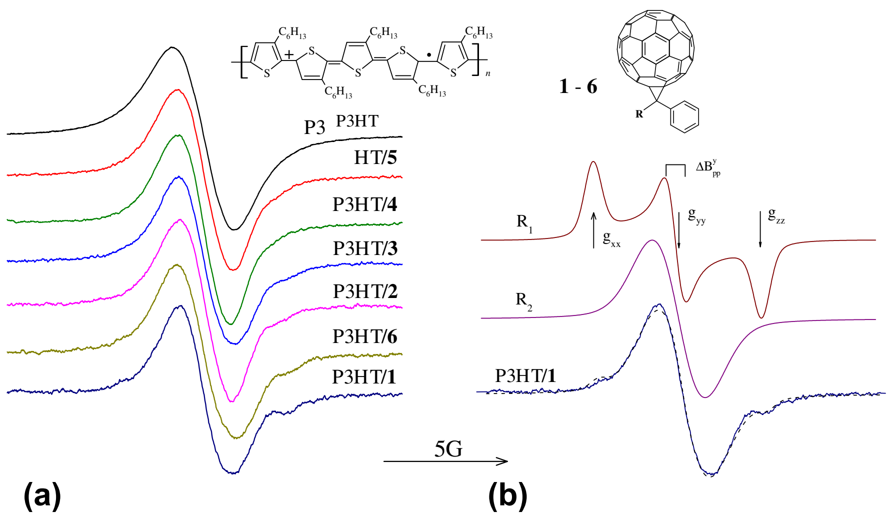

Fig. 1. (a) EPR spectra of the initial P3HT and fullerene-modified samples P3HT/**1**–P3HT/**6** registered at 300 K and $B_1 = 15$ mG. (b) Experimental EPR spectrum of the sample P3HT/**1** (solid line) compared with sum theoretical spectrum (dashed line) of localized R_1 and mobile R_2 polarons calculated from Eqs. (1) and (2) with relative concentration ratio $[R_1]/[R_2] = 0.089$ and $I_L^0/I_G^0 = 0.3$ and 0.2, respectively. The formation of polaron in P3HT is shown schematically. The magnetic resonance parameters measured are also shown.

3. Results and discussion

3.1. Magnetic resonance parameters

No EPR signal was found in pure fullerene derivatives at the 3 cm waveband in the whole temperature range. Using 3 cm waveband EPR, the initial P3HT sample demonstrates a Lorentzian exchange-narrowed, nearly symmetrical line with effective $g_{\text{eff}} = 2.0029$ (Fig. 1). As in the case of regioregular P3AT with longer side chains [18,19], this can be interpreted as stabilization in the polymer of mobile polarons during synthesis and/or its treating by oxygen in the air. As the sample is modified by fullerene, two additional lateral lines appear in its spectrum. This fact is evidence for the localization of part of the polarons, probably at cross-bonds and/or at the ends of polymer chains during such a modification. The intensity of these components decreases in the series

P3HT/**1** → P3HT/**6** → P3HT/**2** → P3HT/**3** → P3HT/**4** → P3HT/**5**.

In order to determine more correctly and completely such main magnetic resonance parameters as the g-tensor terms, peak-to-peak linewidth ΔB_{pp} and paramagnetic susceptibility χ, one should model the EPR spectra of paramagnetic centers (PCs) stabilized in the samples. It is supposed that the first derivative of the effective spectrum $G^{\mid}(B)$ of localized and mobile polarons is characterized by inhomogeneously broadened and motionally narrowed EPR spectra with Gaussian $G_G^{\mid}(B)$ and Lorentzian $G_L^{\mid}(B)$ distributions, respectively [20]

$$G^{\mid}(B) = G_G^{\mid}(B) + G_L^{\mid}(B) = I_G^0 \frac{\sqrt{e}(B - B_0)}{\Delta B_{\text{pp}}} \cdot \exp\left[-\frac{2(B - B_0)^2}{\Delta B_{\text{pp}}^2}\right] + I_L^0 \frac{16(B - B_0)}{9\Delta B_{\text{pp}}} \cdot \left[1 + \frac{4(B - B_0)^2}{3\Delta B_{\text{pp}}^2}\right]^{-2} \qquad (1)$$

The deviation from the g-factor for the free electron ($g_e = 2.00232$) of the g-factor of PCs in such conjugated π-electron systems is due to the non-compensated orbital momentum, which induces an additional magnetic field. The g-tensor terms are expressed by [20]

$$g_{ii} = g_e\left(1 + \frac{\lambda_s \rho_s(0)}{\Delta E_{nj}}\right) \qquad (2)$$

where $\rho_s(0)$ is the spin density on the sulfur nucleus, $\lambda_s = 0.047$ eV [21] is the constant of the spin–orbit interaction of the electron spin with the sulfur nucleus, and ΔE_{nj} is the energy of the electron excitation from the ground orbit to nearest π^* and σ^* orbits. The orbital moment due to direct π–π^* excitation is negligible and shows up on the neighboring C atoms only. However, the g-factor anisotropy is induced by additional fields along the x and y-directions within the plane of the σ skeleton and not along the perpendicular z-direction. For sulfur-containing organic solids, appropriate $\Delta E_{n\pi^*}$ lies near 2.6 eV [22,23] and $\Delta E_{n\sigma^*}$ lies near 15.6 eV [24]. In these systems, each unpaired electron is localized on the sulfur atom, so that their isotropic g-factor lies near 2.018–2.200. The small shift of the effective g-factor of the samples studied from g_e shows that a spin is delocalized in these systems at least on two tens of sulfur sites.

Computer simulation shows that two types of PCs are indeed stabilized in the samples, namely, polarons localized at cross-bonds or/and on the short π-conjugated polymer chains R_1 with $g_{xx} = 2.00493$, $g_{yy} = 2.00301$, $g_{zz} = 2.00098$, and linewidth $\Delta B_{\text{pp}} = 0.66$ G, and a polaron moving along the main π-conjugated polymer chain R_2 with $g_{xx} = g_{yy} = g_{zz} = 2.00292$, and $\Delta B_{\text{pp}} = 2.15$ G. The principal x-axis is chosen parallel to the longest molecular c-axis; the y-axis lies in the thiophene rings plane, and the z-axis is perpendicular to the x and y-axes. The best fit of the R_1 signal was achieved using nearly Gaussian line shape, which means that the transitions are inhomogeneously broadened, mainly as a result of unresolved hyperfine interaction of unpaired spin with protons. Simulated spectra of PCs R_1 and R_2 are also shown in Fig. 1. The effective g-factor of the PCs R_1, $g_{\text{eff}} = 1/3\Sigma g_{ii}$, lies near that of the PCs R_2. This fact supports the supposition made above about the nature of PCs. Spin concentration ratio $[R_1]/[R_2]$ lies near 0.089 for P3HT/**1** and decreases for other compounds (see Fig. 1). Note that the existence of such polarons with different relaxation and dynamics was also determined in other conjugated polymers [25].

3.2. Paramagnetic susceptibility

The effective spin susceptibility of the samples χ is shown in Fig. 2 as a function of temperature. It is seen from Fig. 2 that this parameter depends not only on the temperature, but also on the structure of a fullerene derivative. This value increases on treating the P3HT by fullerene derivatives **1** and **2** and then returns to the previous value in the case of the **3–6** fullerene derivatives (Fig. 2).

Generally, the temperature-dependent static paramagnetic susceptibility of N_s localized and N_e mobile polarons with $S = \frac{1}{2}$ consists of two appropriate parts. The first contribution should follow the Curie law

$$\chi_s(T) = \frac{N_s \mu_{\text{eff}}^2}{3k_B T} \tag{3}$$

where $\mu_{\text{eff}} = \mu_B g\sqrt{S(S+1)}$ is the effective magneton, μ_B is the Bohr magneton, and k_B is the Boltzmann constant.

The samples studied demonstrate more complex temperature dependence for their own spin susceptibility (Fig. 2). The analysis shows that this value cannot be described in terms of the model of interacting spins proposed by Raghunathan et al. [26] for doped organic conductors, regioregular P3HT among them [27]. In order to interpret the experimental data obtained, one should also consider the term of susceptibility due to Q1D mobile polarons characterized by mid-gap energy $E_g = 2E_a$ near the Fermi level [28,29]

$$\chi_e(T) = 2\chi_e^0 \int_{\Omega}^{\infty} \frac{x}{\sqrt{x^2 - \Omega^2}} \frac{e^x}{(1+e^x)^2} dx = \chi_e^0 \begin{cases} \sqrt{\Omega}\exp(1-\Omega) & \text{at } \Omega \geqslant 4 \\ (1 - 0.21\Omega^2) & \text{at } \Omega \leqslant 1/4 \end{cases} \tag{4}$$

where $\Omega = E_a/k_B T$.

The analysis shows that the E_a value evaluated using the high-temperature limit of Eq. (4) is too large (3–20 eV), so to interpret the data one should use the other limit of Eq. (4). In this case, the spin susceptibility of mobile polarons is characterized by activation law and, in addition, the $T^{-1/2}$ factor appears in its temperature dependence.

Indeed, Fig. 2 shows that the experimental data obtained for all the polymer systems are fitted well by the following combination of Eqs. (3) and (4):

$$\chi(T) = \frac{k_1}{T} + k_2\sqrt{\frac{E_a}{k_B T}}\exp\left(1 - \frac{E_a}{k_B T}\right) \tag{5}$$

with appropriate coefficients k_1 and k_2 and the E_a summarized in Table 1.

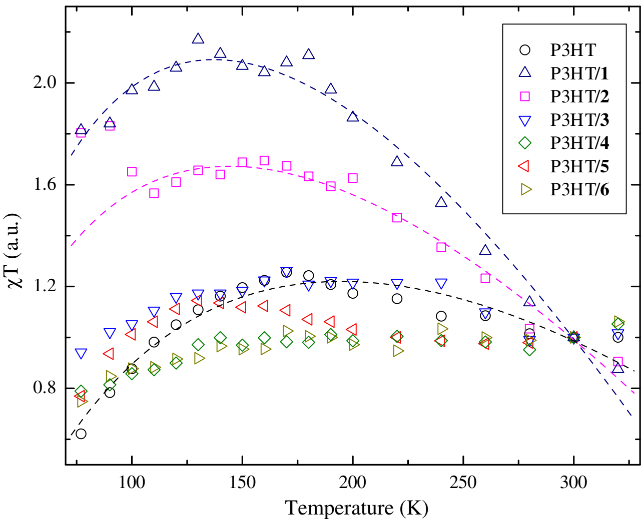

Fig. 2. χT vs T dependences obtained for the initial P3HT and fullerene-modified samples P3HT/**1**–P3HT/**6**. Vertical dashed lines show the dependences calculated from Eq. (5) with $E_a = 2.0$, 1.9 and 4.0 meV, respectively.

3.3. EPR linewidth

The effective EPR linewidth of PCs stabilized in the initial and fullerene-treated P3HT samples is presented in Fig. 3 as a function of temperature. One can see that this value decreases distinctly on P3HT fullerene treatment, but changes weakly within the polymer/fullerene series. This value is determined mainly by the spin–spin relaxation time T_2, but there are several relaxation processes which cause the shortening of T_2 and hence the broadening of the EPR line. One of them is spin relaxation on the lattice phonons with time T_1, which shortens the lifetime of a spin state and therefore broadens the line. If one represents all the other relaxation processes by the time $T_2^{|}$, one can write for effective peak-to-peak width ΔB_{pp} of a Lorentzian line [30]

$$\Delta B_{pp} = \frac{1}{\sqrt{3}\gamma_e} \cdot \frac{1}{T_2} = \frac{1}{\sqrt{3}\gamma_e} \cdot \left(\frac{1}{T_2^{|}} + \frac{1}{2T_1}\right) \tag{6}$$

where γ_e is the gyromagnetic ratio for the electron.

For an isolated spin, there are two main contributions to the $1/T_2^{|}$ term of Eq. (6), namely spin dipole–dipole ω_d and hyperfine ω_h interactions [31]. However, if the spin is movable or exchange interacts with other spins with ω_{ex} exceeding both the ω_d and ω_h values, its line becomes motional narrowed and [32]

$$\frac{1}{T_2^{|}} = \frac{10\omega_d^2 + 3\omega_h^2}{3\omega_{ex}} \cdot = \frac{\gamma_e}{3B_{ex}} \cdot \left[51\mu_{\text{eff}}^2 n_e^2 + A^2 I(I+1)\right] \tag{7}$$

Table 1
Parameters E_a, E_{dd} and E_b (all in meV) determined from Eqs. (5), (8), and (13), respectively, as well as the D_{1D} (in 10^{11} rad s^{-1}) and D_{1D}/D_{3D} values determined from Eqs. (11) and (12) at room temperature for the initial P3HT and fullerene-treated samples P3HT/**1**–P3HT/**6** with side chains *R*

Sample	*R*	E_a	E_{dd}	E_b	D_{1D}	D_{1D}/D_{3D}
P3HT	–	4.0	5.0	25.3	3.3	12
P3HT/**1**	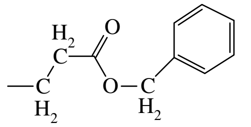	2.0	4.4	23.8	5.4	16
P3HT/**2**	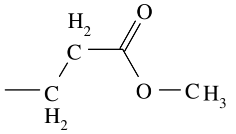	1.9	4.3	19.8	6.0	32
P3HT/**3**	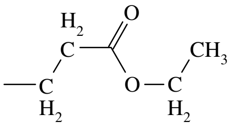	2.0	4.6	10.9	7.7	77
P3HT/**4**	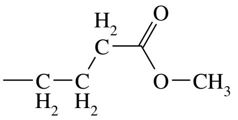	1.4	3.8	2.7	8.6	71
P3HT/**5**	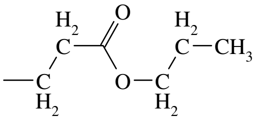	1.7	3.9	0.9	5.2	18
P3HT/**6**	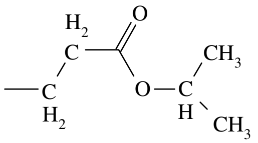	0.2	3.7	9.9	22	1300

where B_{ex} is the additional magnetic field arising as a result of spin motion, n_e is the spin concentration, A is the hyperfine constant, and I is the nuclear spin.

The diffusing of polarons along and between chains of conjugated polymers is studied using the Bloch–Hasegawa equations [29]. The linewidth of such a system spin reservoir is determined mainly by dipole–dipole activation interaction between two types of polarons with activation energy E_{dd}, so that [29,33]

$$\Delta B_{pp}(T) = \Delta B^0_{pp} T^{-1/2} \exp\left(-\frac{E_{dd}}{k_B T}\right) \tag{8}$$

Some dependences calculated from Eq. (8) with different E_{dd} values are also presented in Fig. 3, which shows that the temperature dependences of the linewidth determined from the spectra are described well by the above equation with E_{dd} summarized in Table 1.

3.4. Spin relaxation

As the magnetic term B_1 of microwave irradiation increases, the absorption line of the polarons is broadened, and its intensity I_L changes non-linearly, as shown in Fig. 3. This is due to the steady-state saturation of the whole spin reservoir, allowing one to determine separately the effective T_1 and T_2 values from relations [34]

$$\Delta B_{pp} = \Delta B^{(0)}_{pp} \sqrt{1 + \gamma_e^2 B_1^2 T_1 T_2} \tag{9}$$

$$I_L = I^0_L B_1 (1 + \gamma_e^2 B_1^2 T_1 T_2)^{-3/2} \tag{10}$$

where $\Delta B^{(0)}_{pp} = \sqrt{3}/2\gamma_e T_2$ is the linewidth of the unsaturated line at the $B_1 \to 0$ limit. The relaxation parameters of polarons determined from Eqs. (9) and (10) using such a method are presented in Fig. 4a.

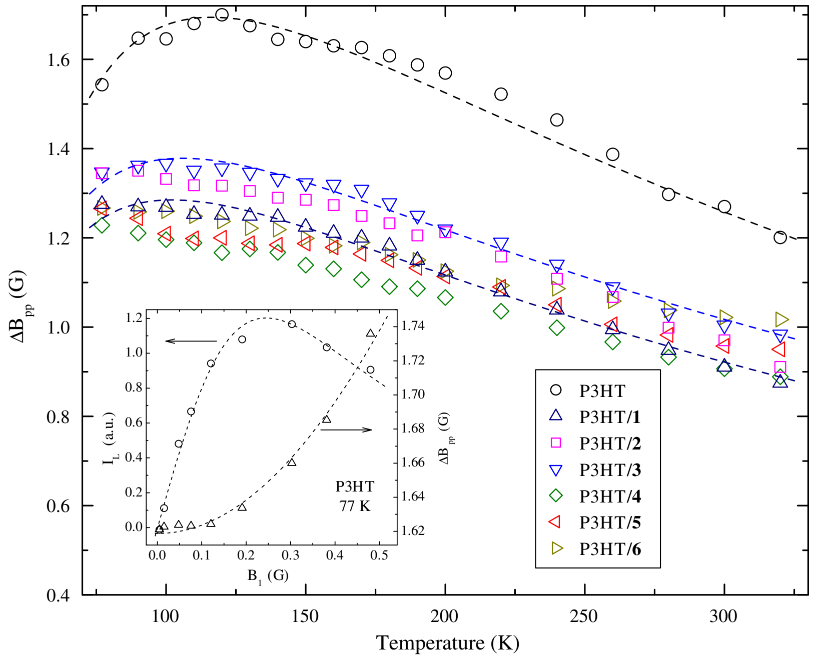

Fig. 3. Peak-to-peak linewidth of the initial P3HT and fullerene-modified samples P3HT/**1**–P3HT/**6** as a function of temperature. The top-to-down dashed lines show the dependences calculated from Eq. (8) with $E_a = 5.0$, 4.6 and 4.4 meV, respectively. In the insert, the change in the line amplitude and width of the initial P3HT sample with the B_1 value at $T = 77$ K as well as the dependences calculated from Eqs. (9) and (10) with $T_1 = 1.2 \times 10^{-6}$ s and $T_2 = 4.1 \times 10^{-8}$ s are shown.

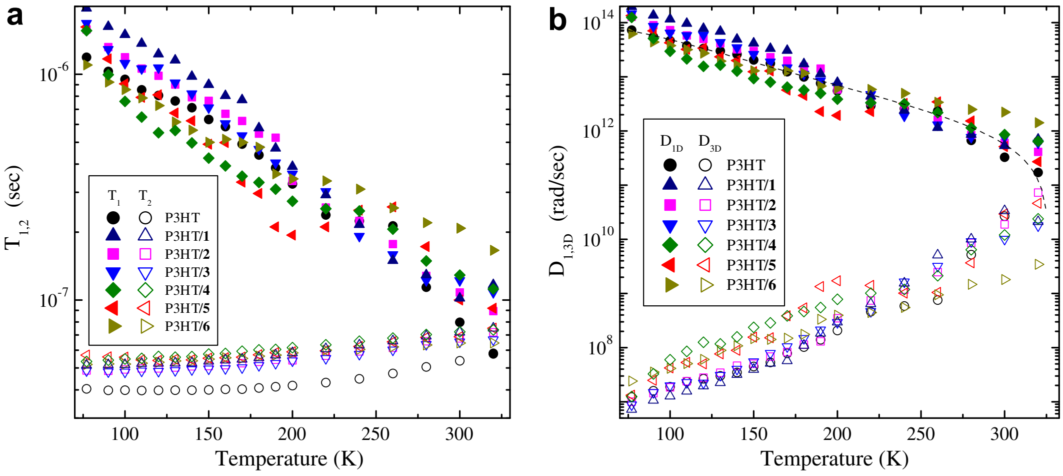

Fig. 4. (a) Temperature dependences of the longitudinal (T_1, filled points) and transversal (T_2, open points) relaxation times determined from Eqs. (9) and (10) as well as (b) the intrachain (D_{1D}, filled points) and interchain (D_{3D}, open points) diffusion coefficients determined from Eqs. (11) and (12) for polarons stabilized in the initial P3HT and fullerene-modified samples P3HT/**1**–P3HT/**6**. The dependence calculated from Eq. (13) with $E_a = 25.3$ meV is also shown as an example by the dashed line.

3.5. Spin dynamics

Part of the polarons diffusing along and between the polymer chains with respective diffusion coefficients D_{1D} and D_{3D} induces an additional magnetic field near another spin, which, in turn, accelerates the electron relaxation of the whole spin ensemble. As the relaxation times of the spins are defined mainly by their dipole–dipole interaction, the following equations can be written [21]:

$$T_1^{-1}(\omega_e) = \langle\omega^2\rangle[2J(\omega_e) + 8J(2\omega_e)] \tag{11}$$

$$T_2^{-1}(\omega_e) = \langle\omega^2\rangle[3J(0) + 5J(\omega_e) + 2J(2\omega_e)] \tag{12}$$

where $\langle\omega^2\rangle = 1/10\gamma_e^4\hbar^2 S(S+1)n\sum_{ij}$ is the constant of a dipole–dipole interaction for powder with n polarons per each monomer and lattice sum $\sum_{ij}, J(\omega_e) = (2D_{1D}^{|}\omega_e)^{-1/2}$ at $D_{1D}^{|} \gg \omega_e \gg D_{3D}$ or $J(0) = (2D_{1D}^{|}D_{3D})^{-1/2}$ at $D_{3D} \gg \omega_e$ is a spectral density function for Q1D motion $D_{1D}^{|} = 4D_{1D}/L^2, \omega_e$ is the resonant angular frequency of the electron spin precession, and L is a factor of spin delocalization over a polaron equal to approximately five monomer units in P3AT [35]. A similar spectral density function was used earlier in the study of spin dynamics in other conjugated polymers [11,25].

Fig. 4b shows how the coefficients D_{1D} and D_{3D} of polaron diffusion in the initial and fullerene-modified samples calculated from Eqs. (11) and (12) at $L \approx 5$ [35] change with temperature. The data obtained show that the D_{1D} value as well as the anisotropy of spin diffusion D_{1D}/D_{3D} tend to increase in the series P3HT → P3HT/**1** → ··· → P3HT/**6** (see Table 1).

The analysis shows that the best interpretation of the $D_{1D}(T)$ dependences presented in Fig. 4 should be interpreted in terms of the motion of small polarons through activation barrier E_b in the Q1D system [36,37]. In this case the D_{1D} value changes with temperature as

$$D_{1D}(T) = D^0_{1D} T^{-4} \exp\left(-\frac{E_b}{k_B T}\right) \qquad (13)$$

Fig. 4 shows that the temperature dependences determined for polaron diffusion along polymer chains in the polymer systems studied are fitted well by Eq. (13), with E_b also presented in Table 1. The activation barrier energies obtained lie near those determined for lattice phonons in other conjugated polymers [25], poly(3-octylthiophene) [19] and P3HT [38] among them.

4. Conclusions

In this work, comparative EPR studies of the magnetic, relaxation and electron dynamics properties of the initial P3HT sample and different P3HT/fullerene composites were performed. The treatment of P3HT with fullerene derivative changed the interaction of polarons with their own microenvironment which in turn changed their magnetic, relaxation and dynamic parameters. The microwave saturation studies allowed all the relaxation parameters of the polarons with different relaxation and mobility formed in these samples to be determined separately.

The effective relaxation times and paramagnetic susceptibility of both types of paramagnetic centers are governed by their dipole–dipole interaction. These parameters as well as the dynamics of mobile polarons depend on the molecular structure of the fullerene derivative. Electronic dynamics can be described in terms of the activation diffusion of small polarons along the polymer chains in the initial and fullerene-modified P3HT. The rate and anisotropy of these dynamics are also governed by the structure of the fullerene derivative and, probably, its donor–acceptor properties. The introduction of the **1**–**6** fullerene derivatives into the polymer matrix changes the polymer dimensionality, which accelerates polaron diffusion along the polymer chain and, therefore, its interaction with the polymer matrix. The fullerene derivative introduces specific states, initiating the localization of part of the mobile polarons.

The data obtained show that the activation barrier E_b crossed by a polaron increases in the order P3HT/**5** → P3HT/**4** → P3HT/**3** → P3HT/**6** → P3HT/**2** → P3HT/**1**. This is accompanied by an increase in concentration of the localized polarons R_1 as well as in the spin susceptibility and spin–lattice relaxation time in the polymer/fullerene system. It seems that such linear side chains in fullerene derivatives **3** (R=–$CH_2CH_2COOCH_2CH_3$), **4** (R=–$CH_2CH_2CH_2COOCH_3$), and **5** (R=–$CH_2CH_2COOCH_2CH_2CH_3$) decrease the activation barrier E_b. Shortening (R=–$CH_2CH_2COOCH_3$ (**2**)) or branching (R=–$CH_2CH_2COOCH(CH_3)_2$ (**6**) or R=–$CH_2CH_2COOCH_2C_6H_5$ (**1**)) of the side chain in the molecule of the fullerene derivative results in higher activation barriers. This can be explained by the complex orientation and conformation effect of the fullerene side substitute (depending, for example, on the relative position and orientation of its –CO–O– group) on the conformation of polymer chains via orientation and, to a lesser degree, dispersion van der Waals forces changing the conformation of the polymer chains. The interaction between mobile or localized polarons characterized by the E_a and E_{dd} values is weaker than their interaction with the polymer lattice phonons characterized by E_b. The introduction of an optimal fullerene derivative leads to the simultaneous decrease in these correlated parameters and also to the acceleration of 1D polaronic diffusion in the P3HT/fullerene samples.

The dynamics of polarons photoinduced in different P3AT/fullerene systems is very interesting not only experimentally, but also theoretically. The authors are carrying out some deeper experimentation with P3HT and other P3AT blended with fullerene derivatives to address these questions in more detail.

Acknowledgements

This work was in part supported by the Russian Foundation for Basic Research (Grant 08-03-00133) and by the Human Capital Foundation (Grant No. 07-136).

References

[1] Shinar J. Organic light emitting devices: a survey. New York: Springer; 2002.

[2] Markvart T, Castaner L. Practical handbook of photovoltaics, fundamentals and applications. Oxford: Elsevier; 2003.

[3] Brabec CJ, Dyakonov V, Parisi J, Sariciftci NS. Organic photovoltaics: concepts and realization. Berlin: Springer Verlag; 2003.

[4] Dimitrakopoulos CD, Mascaro DJ. Org Electron 2001;45:11.

[5] Scotheim TE, Reynolds JR, editors. Handbook of conducting polymers, vols. 1–2. Boca Raton, FL: CRC Press; 2007.

[6] Winokur MJ, Spiegel D, Kim Y, Hotta S, Heeger AJ. Synth Met 1989;28:C419.

[7] Prosa TJ, Winokur MJ, Moulton J, Smith P, Heeger AJ. Macromolecules 1992;25:4364.

[8] Barta P, Niziol S, Leguennec P, Pron A. Phys Rev B 1994;50:3016.

[9] Gill RE, Malliaras GG, Wildeman J, Hadziioannou G. Adv Mater 1994;6:132.

[10] Bao Z, Dodabalapur A, Lovinger AJ. Appl Phys Lett 1996;69:4108.

[11] Mizoguchi K, Kuroda S. Magnetic properties of conducting polymers. In: Nalwa HS, editor. Handbook of organic conductive molecules and polymers, vol. 3. Chichester, New York: John Wiley; 1997. p. 251.
[12] Drees M, Hoppe H, Winder C, Neugebauer H, Sariciftci NS, Schwinger W, et al. J Mater Chem 2005;15:5158.
[13] Al Ibrahim M, Roth HK, Schrödner M, Konkin A, Zhokhavets U, Gobsch G, et al. Org Electron 2005;6:65.
[14] Riedel I, von Hauff E, Parisi H, Martin N, Giacalone F, Dyakonov V. Adv Funct Mater 2005;15:1979.
[15] Krinichnyi VI. 2-mm Wave band EPR spectroscopy of condensed systems. Boca Raton, FL: CRC Press; 1995.
[16] Krinichnyi VI. High field ESR spectroscopy of conductive polymers. In: Schlick S, editor. Advanced ESR methods in polymer research. Hoboken, NJ, New York: John Wiley; 2006. p. 307.
[17] Mayorova JY, Nikitenko SL, Troshin PA, Peregudova SM, Peregudov AS, Kaplunov MG, et al. Mendeleev Commun 2007;17:175.
[18] Sensfuss S, Konkin A, Roth H-K, Al-Ibrahim M, Zhokhavets U, Gobsch G, et al. Synth Met 2003;137:1433.
[19] Krinichnyi VI, Roth H-K. Appl Magn Reson 2004;26:395.
[20] Weil JA, Bolton JR, Wertz JE. Electron paramagnetic resonance: elementary theory and practical applications. New York: Wiley-Interscience; 2007.
[21] Carrington F, McLachlan AD. Introduction to magnetic resonance with application to chemistry and chemical physics. New York: Harper & Row; 1967.
[22] Cameron TS, Haddon RC, Mattar SM, Parsons S, Passmore J, Ramirez AP. J Chem Soc, Dalton Trans 1992:1563.
[23] Bock H, Rittmeyer P, Krebs A, Schultz K, Voss J, Kopke B. Phosphorus Sulfur Silicon Relat Elem 1984;19:131.
[24] Krinichnyi VI, Roth H-K, Schrödner M. Appl Magn Reson 2002;23:1.
[25] Krinichnyi VI. Synth Met 2000;108:173.
[26] Raghunathan A, Kahol PK, Ho JC, Chen YY, Yao YD, Lin YS, et al. Phys Rev B 1998;58:R15955.
[27] Kahol PK, McCormick BJ, Epstein AJ, Pandey SS. Synth Met 2003;135:343.
[28] Jonston DC. Phys Rev Lett 1984;52:2049.
[29] Barnes SE. Adv Phys 1981;30:801.
[30] Wertz JE, Bolton JR. Electron spin resonance: elementary theory and practical applications. London: Chapman & Hall; 1986.
[31] Altshuler SA, Kozirev BM. Electron paramagnetic resonance. New York: Academic Press; 1964.
[32] Kubo R, Tomita K. J Phys Soc Jpn 1954;9:888.
[33] Atsarkin VA, Demidov VV. J Exp Theor Phys 1998;86:572.
[34] Poole ChP. Electron spin resonance: a comprehensive treatise on experimental techniques. New York: John Wiley; 1983.
[35] Devreux F, Genoud F, Nechtschein M, Villeret B. On polaron and bipolaron formation in conducting polymers. In: Kuzmany H, Mehring M, Roth S, editors. Electronic properties of conjugated polymers. Springer series in solid state sciences, vol. 76. Berlin: Springer Verlag; 1987. p. 270.
[36] Long AR. Adv Phys 1982;31:553.
[37] Patzsch J, Gruber H. Small polarons in polymeric polytetrathiafulvalenes (PTTF). In: Kuzmany H, Mehring M, Roth S, editors. Electronic properties of polymers. Springer series in solid state sciences, vol. 107. Berlin: Springer Verlag; 1992. p. 121.
[38] Chiguvare Z, Dyakonov V. Phys Rev B 2004;70:235207.